ISSN 1674-1056
http://cpb.iphy.ac.cn
http://iopscience.iop.org/cpb
中国物理 B
Chinese Physics
中国物理
Chinese Physics B

Discrete state space method and modal extension method based impact sound synthesis model

Xu-Hua Tian(田旭华), Ke-An Chen(陈克安), Yan-Ni Zhang(张燕妮), Han Li(李晗), Jian Xu(胥健)

Citation: Chin. Phys. B . 2018, 27(11): 114302. **doi:** 10.1088/1674-1056/27/11/114302

Journal homepage: http://cpb.iphy.ac.cn; http://iopscience.iop.org/cpb

What follows is a list of articles you may be interested in

Tunable coupling of a hybrid plasmonic waveguide consisting of two identical dielectric cylinders and a silver film

Benli Wang(王本立) , Han Liang(梁涵) , and Jiafang Li(李家方)

Chin. Phys. B .2017 26 (11): 114103 **doi:** 10.1088/1674-1056/26/11/114103

Structure-dependent behaviors of diode-triggered silicon controlled rectifier under electrostatic discharge stress

Li-Zhong Zhang(张立忠), Yuan Wang(王源)†, and Yan-Dong He(何燕冬)

Chin. Phys. B, 2016,25 (12) 128501 **doi:** 10.1088/1674-1056/25/12/128501

SPECIAL TOPIC — 80th Anniversary of Northwestern Polytechnical University (NPU)

Discrete state space method and modal extension method based impact sound synthesis model*

Xu-Hua Tian(田旭华), Ke-An Chen(陈克安)†, Yan-Ni Zhang(张燕妮), Han Li(李晗), and Jian Xu(胥健)

Department of Environmental Engineering, School of Marine Science and Technology, Northwestern Polytechnical University, Xi'an 710072, *China*

(Received 20 June 2018; revised manuscript received 1 October 2018; published online 8 October 2018)

The efficient and accurate synthesis of physical parameter-controllable impact sounds is essential for sound source identification. In this study, an impact sound synthesis model of a cylinder is proposed based on discrete state space (DSS) method and modal extension method (MEM). This model is comprised of the whole three processes of the physical interaction, i.e., the Hertz contact process, the transient structural response process, and the sound radiation process. Firstly, the modal expanded DSS equations of the contact system are constructed and the transient structural response of the cylinder is obtained. Then the impact sound of the cylinder is acquired using improved discrete Raleigh integral. Finally, the proposed model is verified by comparing with existing models. The results show that the proposed impact sound synthesis model is more accurate and efficient than the existing methods and easy to be extended to the impact sound synthesis of other structures.

Keywords: impact sound synthesis, discrete state space, contact force

PACS: 43.40.kd, 43.50.Pn **DOI:** 10.1088/1674-1056/27/11/114302

1. Introduction

Radiated sounds in our daily life usually vary with the physical parameters of vibrating structures. These physical parameters include size, shape, and material, as well as stimuli and radiation condition.[1] Investigating the relationships between physical parameters of structures and sound features is meaningful and attractive in the field of sound source identification.[2] In order to grasp the most essential features of the vibratory and acoustical problem, sound continua should be created since they can simulate the continuous changes of the physical parameters.[3] Recordings or real sounds are not efficient to create continua since actual physical parameters are in inhomogeneous and disperse distribution.[4,5] By contrast, synthetic sounds, which can precisely control different physical parameters and provide large sets of sound samples, seem more suitable. In previous literatures, the synthesized impact sounds are mainly used in sound source identification studies since they are broadband and carrying most of the information related to physical parameters.[6,7] Thus, the synthesis of impact sound continua becomes the premised issue in the study of sound source identification.

A complete impact sound synthesis model should comprise three processes, the contact process of the hammer and the structure, the vibration response process of the structure, and the sound radiation process. The contact process was substituted by pre-defined contact forces in wave forms of a half sine or two half-Gaussians which rise fast and decay slow in some studies.[5,8] Meanwhile, the other studies used the Hertz contact model, which is closer to the reality compared with pre-defined forces, to stimulate the whole processes of the contact.[9,10] The vibration response and radiation process was usually modeled with basic theoretical derivation, modal expansion method (MEM), finite difference method (FDM), finite element method (FEM), boundary element method (BEM), and combination of the above methods.[9–13] Lambourg (2001) synthesized the vibration response and impact sound through the finite-difference time-domain (FDTD) method and discrete Raleigh integral, but his method had a drawback of low computational efficiency.[9] Lutfi (2001) and McAdams (2010) used simplified models based on Lambourg's method to synthesize the impact sound of bar and plate for subjective judgments, but their models would not be suitable for the accurate-sound-feature extraction since they ignored the information which is not sensitive by the human ears.[10,11] Zhang (2014) proposed FDTD-MEM method and FEM-MEM-BEM method (implemented in LMS Virtual.Lab software) to synthesize impact sound more efficiently than FDTD method under the same precision.[12,13] However, Zhang's methods still suffered from low computational efficiency caused by high order FDTD and large number of finite elements. In addition, Avanzini (2001) put forward a low parameter sound synthesis model, from which the system was constructed by DSS equations discretized through bilinear transform method.[14] The DSS equations are first order with

*Project supported by the National Natural Science Foundation of China (Grant Nos. 11574249 and 11874303) and the Natural Science Basic Research Plan in Shaanxi Province of China (Grant No. 2018JQ1001).

†Corresponding author. E-mail: kachen@nwpu.edu.cn

© 2018 Chinese Physical Society and IOP Publishing Ltd

lower computing cost than high order FDTD equations. Nevertheless, Avanzini's model neglects both stimulus-position information and radiation process, and the model is not accurate due to the bilinear transform method adopted to discrete the state space equations. Although aforementioned methods have advantages respectively in accuracy and efficiency, an efficient and accurate method for sound synthesis still needs to be developed for sound feature identification tasks.

In order to have a simultaneous improvement on the accuracy and the computational efficiency compared to aforementioned methods and ensure the information integrity of the synthesized sounds, an impact sound synthesis model is proposed in this study. The model comprises the Hertz contact process, the vibration response process, and the sound radiation process. And it is firstly built with modal expanded DSS equations. Then the vibration response and radiated sound of the simply-supported cylinder, which is widely used in airplane and ship manufactures, are calculated using two approximate methods (Euler method and trapezoid method). The results show that the proposed sound synthesis model is superior to the existing methods in both accuracy and efficiency. The proposed model can provide a large number of sound samples for the subsequent sound source identification study and it can be extended to other structures with just a few modifications of the modal parameters.

2. Impact sound synthesis model

2.1. Overview of the model

The impact sound synthesis model used in this paper is described briefly in Fig. 1. It comprises the Hertz contact process, the transient structural response process, and the sound radiation process. The Hertz contact process consists of three parts, i.e., the cylinder motion, the hammer motion, and the contact force calculation. By solving the Hertz contact process, the force response and point response can be obtained. The structural response of the whole cylinder surface can be extended from the point response using MEM. In the sound radiation process, the sound field radiated from the cylinder surface is calculated.

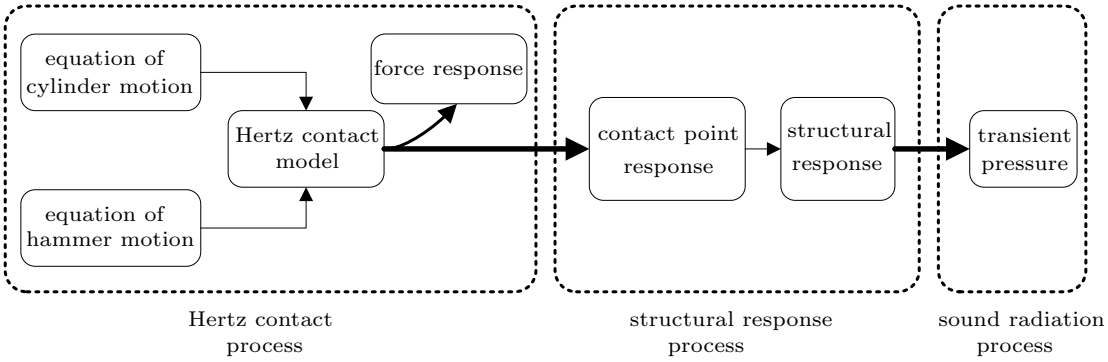


Fig. 1. The sound synthesis model.

2.2. Basic equations

Basic equations of different parts of the sound synthesis model are displayed in the following subsections. They will be discretized and solved in a form of regressive iteration equations in Section 3.

2.2.1. Cylinder motion

In order to decrease the dimension of iterative computation, the equations of the contact system are usually modal expanded using MEM. The modal expanded second order differential equation of the cylinder can be expressed as follows:

$$\ddot{x}_l^{(\mathrm{r})}(t)+\mathrm{g}_l^{(\mathrm{r})}\dot{x}_l^{(\mathrm{r})}(t)+\left[\omega_l^{(\mathrm{r})}\right]^2 x_l^{(\mathrm{r})}(t)=f_l(t), \tag{1}$$

where the superscript (r) represents the resonant cylinder, $x_l^{(\mathrm{r})}(t)$, $\mathrm{g}_l^{(\mathrm{r})}$, $\omega_l^{(\mathrm{r})}$, and $f_l(t)$ are respectively the modal amplitude, the modal damping, the modal angular frequency, and the modal forces of the l-th mode. By defining φ_l as the l-th modal shape of the structure, the terms in Eq. (1) can be described as follows:[15]

$$\begin{cases} g_l^{(\mathrm{r})}=2\zeta_l\omega_l,\ \ f_l(t)=\varphi_l^{\mathrm{T}}\cdot\boldsymbol{f}(t),\ \ M_l^{(\mathrm{r})}=\rho h\Delta S\cdot\varphi_{mn}^{\mathrm{T}}\varphi_{mn}, \\ \varphi_l=\dfrac{1}{\sqrt{M_l}}\varphi_{mn}=\dfrac{1}{\sqrt{M_l}}\sin(k_m z)\cos(n\theta), \end{cases} \tag{2}$$

where k_m, n, θ, ρ, and h stand for the axial wave number, the circumferential order, the circumferential angle, the mass density, and the thickness of the cylinder, respectively. ζ_l denotes the l-th (corresponding to the (m,n) order mode of the cylinder) modal damping ratio. The total displacement $w(x_p,t)$ of point x_p can be calculated according to the modal analysis theory as

$$w(x_p,t)=\sum_l x_l^{(\mathrm{r})}(t)\,\varphi_l(x_p), \tag{3}$$

where $\varphi_l(x_p)$ is the positional coefficient of the l-th modal shape at point x_p.

2.2.2. Hammer motion

Assuming the contact process is on the horizontal direction, the equation of hammer motion can be described as

$$M^{(\mathrm{h})}\ddot{x}^{(\mathrm{h})}(t) = -f(t), \tag{4}$$

where the superscript (h) represents the hammer, and $f(t)$ is the contact force.

2.2.3. Contact force

Contact force (or impact force) is one of the crucial clues associated with the physical parameters of the hammer, such as the hardness.[16] As mentioned in Section 1, contact forces are mainly in forms of pre-defined force and synthesized Hertz contact force. The Hertz contact theory can simulate the whole process of the collision and it is more close to the reality compared with pre-defined force. So the contact force model proposed by Hunt and Crossley is introduced as follows:[17]

$$\begin{aligned} f(t) &= f(\Delta x(t), \Delta v(t)) \\ &= k\Delta x(t)^{\alpha} + \lambda \Delta x(t)^{\alpha} \cdot \Delta v(t), \quad \Delta x, \Delta v \geq 0, \end{aligned} \tag{5}$$

where k is the contact stiffness, λ and α denote the damping coefficient and the index, respectively, and they are set to $0.6k$ and 3.8 following Avanzini's configurations. $\Delta x(t)$ and $\Delta v(t)$ represent the relative displacement and the relative velocity between the hammer and the cylinder respectively

$$\begin{cases} \Delta x(t) = x^{(\mathrm{h})}(t) - w(x_p, t), \\ \Delta v(t) = v^{(\mathrm{h})}(t) - \dot{w}(x_p, t). \end{cases} \tag{6}$$

2.2.4. Sound radiation

The free field sound radiation can be calculated using the Raleigh integral[9,18]

$$p(\bar{r}, t) = \int_S \frac{\rho_0 \dot{v}(t - \bar{r}/c_0)}{2\pi \bar{r}} \mathrm{d}s = \int_S \frac{\rho_0 \ddot{x}(t - \bar{r}/c_0)}{2\pi \bar{r}} \mathrm{d}s, \tag{7}$$

where $\bar{r}$ is the distance between the receiving point and the surface of the structure; ρ_0 and c_0 stand for the density and the sound speed in air, respectively.

3. Structural response based on DSS and MEM

3.1. Theory

In order to improve the accuracy and the computational efficiency of aforementioned methods, we propose an accurate DSS and MEM based method to calculate the structural response of the cylinder. The modal expanded DSS equation of Eq. (1) can be expressed as

$$\dot{\boldsymbol{x}}^{(\mathrm{r})}(t) = \boldsymbol{A}\boldsymbol{x}^{(\mathrm{r})}(t) + \boldsymbol{B}\boldsymbol{u}(t), \tag{8}$$

where

$$\boldsymbol{x}^{(\mathrm{r})}(t) = \begin{bmatrix} \boldsymbol{x}_1^{(\mathrm{r})}(t) \\ \boldsymbol{x}_2^{(\mathrm{r})}(t) \\ \boldsymbol{x}_3^{(\mathrm{r})}(t) \\ \vdots \end{bmatrix}; \quad \boldsymbol{x}_l^{(\mathrm{r})}(t) = \begin{Bmatrix} x_l^{(\mathrm{r})}(t) \\ \dot{x}_l^{(\mathrm{r})}(t) \end{Bmatrix};$$

$$\boldsymbol{A} = \begin{bmatrix} \boldsymbol{A}_1 & & & \\ & \boldsymbol{A}_2 & & \\ & & \boldsymbol{A}_3 & \\ & & & \ddots \end{bmatrix}; \quad \boldsymbol{B} = \begin{bmatrix} \boldsymbol{B}_1 \\ \boldsymbol{B}_2 \\ \boldsymbol{B}_3 \\ \vdots \end{bmatrix};$$

$$\boldsymbol{A}_l = \begin{bmatrix} 0 & 1 \\ -\lambda_l & -2\zeta_l\omega_l \end{bmatrix}; \quad \boldsymbol{B}_l = \begin{bmatrix} 0 & \cdots & 0 \\ \psi_l(x_1) & \cdots & \psi_l(x_m) \end{bmatrix};$$

$$\boldsymbol{u}(t) = [f_1(t) \cdots f_m(t)]^{\mathrm{T}}.$$

Instead of discretizing the equations directly as Avanzini did,[14] we solve Eq. (8) and acquire an accurate solution before the discretization operation. The accurate solution of Eq. (8) is shown as follows:[19]

$$\boldsymbol{x}^{(\mathrm{r})}(t) = \mathrm{e}^{\boldsymbol{A}(t-t_0)}\boldsymbol{x}^{(\mathrm{r})}(t_0) + \int_{t_0}^{t} \boldsymbol{B}\cdot\boldsymbol{u}(\tau)\,\mathrm{e}^{\boldsymbol{A}(t-\tau)}\,\mathrm{d}\tau, \tag{9}$$

where the first term on the right hand side is the solution of the free vibration, and the second term is the forced vibration solution (also called Duhamel integral), and $\tau \in [t_0, t]$ is the period considered. The discrete form of Eq. (9) can be found in Ref. [19]

$$\boldsymbol{x}^{(\mathrm{r})}(n) = \mathrm{e}^{\boldsymbol{A}T}\boldsymbol{x}^{(\mathrm{r})}(n-1) + \boldsymbol{\Theta}\boldsymbol{B}\bar{\boldsymbol{u}}(\tau)/F_{\mathrm{s}}, \tag{10}$$

where $\bar{\boldsymbol{u}}(\tau)$ is the average value in $\tau \in [nT - T, nT]$, F_{s} is the sampling rate, and $\boldsymbol{\Theta}$ equals to $\boldsymbol{I} + \sum_{i=1}^{\infty} \frac{(\boldsymbol{A}/F_{\mathrm{s}})^i}{(i+1)!}$. The upper limit of i can be set to 5–10 since $\frac{(\boldsymbol{A}/F_{\mathrm{s}})^i}{(i+1)!}$ is negligible when i exceeds 5. To improve the iterative efficiency, equation (10) is divided into two iterative formulas

$$\begin{bmatrix} \boldsymbol{X}^{(\mathrm{r})}(n) \\ \boldsymbol{V}^{(\mathrm{r})}(n) \end{bmatrix} = \begin{bmatrix} \mathrm{e}^{\boldsymbol{A}'T}\boldsymbol{X}^{(\mathrm{r})}(n-1) \\ \mathrm{e}^{\boldsymbol{A}'T}\boldsymbol{V}^{(\mathrm{r})}(n-1) \end{bmatrix} + \begin{bmatrix} \boldsymbol{\Theta}'\boldsymbol{B}'\bar{\boldsymbol{u}}(\tau)/F_{\mathrm{s}} \\ \boldsymbol{\Theta}'\boldsymbol{B}'\bar{\boldsymbol{u}}(\tau)/F_{\mathrm{s}} \end{bmatrix}, \tag{11}$$

where $\boldsymbol{X}(n)$ and $\boldsymbol{V}(n)$ are respectively the displacement amplitude vector and the velocity amplitude vector of all the modes considered. $\mathrm{e}^{\boldsymbol{A}'T}$ and $\boldsymbol{\Theta}'\boldsymbol{B}'/F_{\mathrm{s}}$ are pre-calculated before the iteration process since they are time independent. The quantities $\boldsymbol{A}'$, $\boldsymbol{B}'$, and $\boldsymbol{\Theta}'$ are expressed as follows:

$$\boldsymbol{A}' = \begin{bmatrix} 0 & 1 & -\lambda_1 & -2\zeta\omega_1 \\ 0 & 1 & -\lambda_2 & -2\zeta\omega_2 \\ 0 & 1 & -\lambda_3 & -2\zeta\omega_3 \\ \vdots & \vdots & \vdots & \vdots \end{bmatrix},$$

$$\boldsymbol{B}' = \begin{bmatrix} \psi_1(x_1) & \psi_1(x_2) & \cdots & \psi_1(x_m) \\ \psi_2(x_1) & \psi_2(x_2) & \cdots & \psi_2(x_m) \\ \psi_3(x_1) & \psi_3(x_2) & \cdots & \psi_3(x_m) \\ \vdots & \vdots & \cdots & \vdots \end{bmatrix}, \tag{12}$$

$$\boldsymbol{\Theta}' = \boldsymbol{I}' + \sum_{i=1}^{\infty} \frac{(\boldsymbol{A}'/F_{\mathrm{s}})^i}{(i+1)!}, \tag{13}$$

where $\boldsymbol{I}'$ and $(\boldsymbol{A}')^i$ should be redefined as

$$\boldsymbol{I}' = \begin{bmatrix} 1 & 0 & 0 & 1 \\ 1 & 0 & 0 & 1 \\ 1 & 0 & 0 & 1 \\ \vdots & \vdots & \vdots & \vdots \end{bmatrix}, \tag{14}$$

$$\begin{cases} \boldsymbol{A}' = [\boldsymbol{A}'(1)\ \boldsymbol{A}'(2)\ \boldsymbol{A}'(3)\ \boldsymbol{A}'(4)], \\ (\boldsymbol{A}')^2 = \begin{bmatrix} \boldsymbol{A}'(1)\circ\boldsymbol{A}'(1)+ & \boldsymbol{A}'(1)\circ\boldsymbol{A}'(2)+ & \boldsymbol{A}'(3)\circ\boldsymbol{A}'(1)+ & \boldsymbol{A}'(3)\circ\boldsymbol{A}'(2)+ \\ \boldsymbol{A}'(2)\circ\boldsymbol{A}'(3) & \boldsymbol{A}'(2)\circ\boldsymbol{A}'(4) & \boldsymbol{A}'(4)\circ\boldsymbol{A}'(3) & \boldsymbol{A}'(4)\circ\boldsymbol{A}'(4) \end{bmatrix}, \\ (\boldsymbol{A}')^3 = \begin{bmatrix} (\boldsymbol{A}')^2(1)\circ\boldsymbol{A}'(1)+ & (\boldsymbol{A}')^2(1)\circ\boldsymbol{A}'(2)+ & (\boldsymbol{A}')^2(3)\circ\boldsymbol{A}'(1)+ & (\boldsymbol{A}')^2(3)\circ\boldsymbol{A}'(2)+ \\ (\boldsymbol{A}')^2(2)\circ\boldsymbol{A}'(3) & (\boldsymbol{A}')^2(2)\circ\boldsymbol{A}'(4) & (\boldsymbol{A}')^2(4)\circ\boldsymbol{A}'(3) & (\boldsymbol{A}')^2(4)\circ\boldsymbol{A}'(4) \end{bmatrix}, \\ \cdots \end{cases} \tag{15}$$

where "$\circ$" is the Hadamard product, i.e., the product of elements at the same position of the matrixes.

Accordingly, the DSS equations of the hammer and the contact model can be described as

$$\begin{cases} \dot{x}^{(\mathrm{h})}(n) = \dot{x}^{(\mathrm{h})}(n-1) - \bar{\boldsymbol{u}}(\tau)/F_{\mathrm{s}}m^{(\mathrm{h})}, \\ x^{(\mathrm{h})}(n) = -\sum_{j=1}^{n}\dot{x}^{(\mathrm{h})}(j)/F_{\mathrm{s}}, \end{cases} \tag{16}$$

$$\begin{cases} f(n) = f(\Delta x(n), \Delta v(n)) = k\Delta x(n)^{\alpha} + \lambda\Delta x(n)^{\alpha}\cdot\Delta v(n), \\ \begin{bmatrix} \Delta x(n) \\ \Delta v(n) \end{bmatrix} = \begin{bmatrix} x^{(\mathrm{h})}(n) \\ v^{(\mathrm{h})}(n) \end{bmatrix} - \begin{bmatrix} \sum_l X_l^{(\mathrm{r})}(n)\,\varphi_l(x_p) \\ \sum_l V_l^{(\mathrm{r})}(n)\,\varphi_l(x_p) \end{bmatrix}, \end{cases} \tag{17}$$

where $\bar{\boldsymbol{u}}(\tau)$ can be approximated by the Euler method ($\bar{\boldsymbol{u}}(\tau) = \boldsymbol{u}(n-1)$) or the trapezoid method ($\bar{\boldsymbol{u}}(\tau) = \frac{1}{2}(\boldsymbol{u}(n)+\boldsymbol{u}(n-1))$). In general, the trapezoid method has a better accuracy in approaching the velocity gradient than the Euler method. However, the trapezoid method is more complex since $\boldsymbol{u}(n)$ and $\boldsymbol{x}^{(\mathrm{r})}(n)$ in Eqs. (11) and (16) have instantaneous mutual dependence. Fortunately, K method proposed by Borin[20] could be introduced to calculate $\boldsymbol{u}(n)$ in each time step with a few steps of Newton–Raphson iterations. Detail information about K method used in this study can be found in Ref. [15].

By solving Eqs. (11) and (15)–(17), we can obtain the transient displacement and velocity responses of the driven point. According to modal analysis theory, the responses of driven point $x_p(t)$ and any other point $x_A(t)$ on the cylinder surface can be linked together by

$$\begin{cases} x_{l,A}(t) = x_{l,p}(t)\,\dfrac{\varphi_{Al}}{\varphi_{pl}} = x_{l,p}(t)\,T_{pAl}, \\ v_{l,A}(t) = v_{l,p}(t)\,\dfrac{\varphi_{Al}}{\varphi_{pl}} = v_{l,p}(t)\,T_{pAl}, \end{cases} \quad \text{for } \varphi_{pl} \neq 0, \tag{18}$$

where T_{pAl} is the transfer coefficient between different points. Thus, the l-th structural response of the whole cylinder can be calculated through Eq. (18). The driven point must be on the nodal line of some modes, which may cause unexpected high value of $1/\varphi_{pl}$. Therefore, T_{pAl} is weighed with a coefficient which equals to 0 when φ_{pl} is smaller than a certain threshold (0.01, for the proposed model) and 1 otherwise.

3.2. Results and validation

The parameters of the contact system are given in Table 1. Besides, the initial displacement and velocity are respectively -10^4 m and 2 m/s, and the driven point is located at $x_p(r,\theta,z) = (0.4, 0, 0.08)$. A total of 746 modal frequencies below 5000 Hz are considered in the range of 30×30 orders. The sample rate is set to 40000 Hz to ensure the resolution of temporal contact force.

Table 1. Physical parameters of the system.

Structure	Physical parameters	Value	Unit
Cylinder	length	1.2	m
	radius	0.4	m
	thickness	0.003	m
	Young's modular	2.1×10^{11}	GPa
	Poison ratio	0.3	–
	density	7850	kg/m^3
	damping ratio	0.5	%
Hammer	mass	10^{-3}	kg
	contact stiffness	0.5×10^{11}	GPa

3.2.1. Results

The temporal contact force and velocity response of the cylinder from different approximate methods are displayed in Figs. 2 and 3, respectively. The contact force duration is approximately 3.5 ms. The velocity response at the 27th sampling point is displayed in a two-dimensional color map for better view. The impact point in Fig. 3 is located at $(1, 8)$.

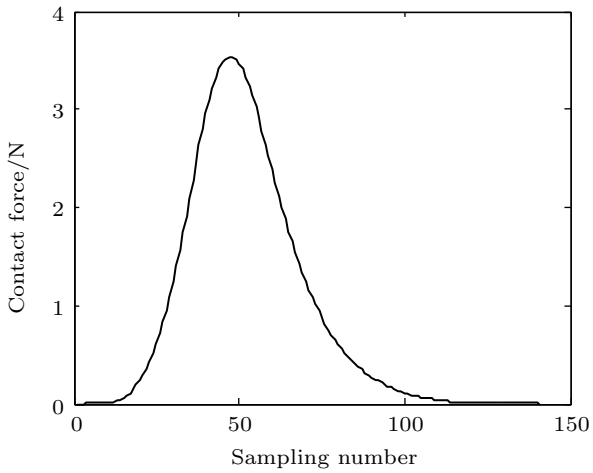


Fig. 2. Temporal contact force.

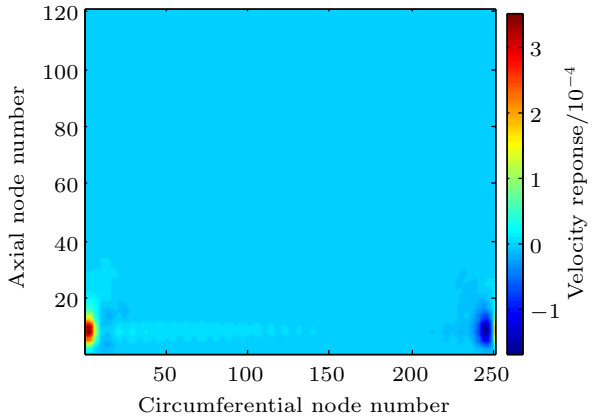


Fig. 3. (color online) Velocity response.

3.2.2. Validation

The FEA software can hardly work out a result under the calculation precision of 5000 Hz since the required element number for the cylinder in Table 1 exceeds 30000. Thus a new method is needed to validate the vibration response. Admittance reflects the properties of the structure, if stimulus is identical, the same admittance dose means the same velocity response (see Eq. (19)). So we can use admittance to validate the transient velocity responses indirectly. The generalized driven-point admittance and theoretical driven-point admittance (in modal analysis) can be expressed respectively as[5,8]

$$Y_p(\omega) = V_p(\omega)/F_p(\omega), \tag{19}$$

$$Y_p(\omega) = \sum_l \frac{-\mathrm{j}\omega\varphi_l^2(\mathrm{x_p})}{m_l(\omega_l^2 - \mathrm{j}\omega\mathrm{g} - \omega^2)}. \tag{20}$$

The driven-point admittance results of different methods are displayed in Fig. 4 in different line styles. Among them, the results of the proposed methods and bilinear transform method are calculated using Eq. (19), meanwhile the theoretical result is calculated from Eq. (20). It is noticed that the driven-point position is considered in all the above methods. The results show that the results of the proposed methods well agree with the theoretical result and the bilinear transform result has obvious deviation in both amplitude and frequency.

The significant deviation of Avanzini's bilinear transform result can be interpreted from two aspects: 1) the Duhamel integral in Eq. (9) is substituted by the oversimplified discrete force in Eq. (4) of Ref. [8], which causes the disagreement of the amplitudes, and 2) the bilinear transform method has a drawback in the frequency reconstruction which causes a shrink of vibration responses in the high frequency domain.

As a complementary validation, the velocity response of a smaller cylinder ($L = 0.3$ $R = 0.1$) calculated using FEM+MEM (realized through the transient modal superposition structural response case in Virtual.Lab software) and proposed method is shown in Fig. 5. The force obtained from Hertz contact process is used as the input force of the transient modal superposition structural response case directly. The result shows a good agreement between the two methods. The small velocity differences between the two methods are due to the resolution difference and modal frequency bais.

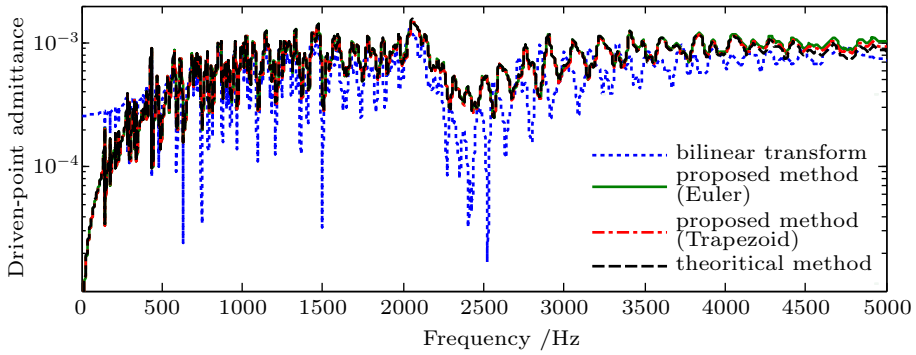


Fig. 4. (color online) Driven-point admittances of different methods.

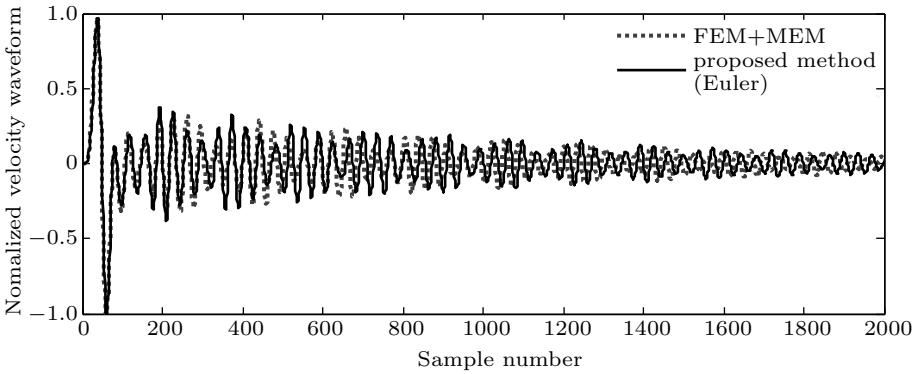


Fig. 5. Contact point velocity of different methods.

3.3. Computational efficiency

The time consumed in different steps of the transient structural response process is displayed in Table 2. All the computations in this paper are accomplished under the same hardware (i7-6700 CPU, 8G DDR4 memory) and software (win10 64bit, matlab2013a) condition. As shown in Table 2, the most time consuming part is the calculation of the cylinder velocity from the driven point velocity since 250×120 nodes need to be calculated in each of the 40000 time intervals. Nevertheless, the total time for driven point response calculation is less than 1 s for the proposed methods.

Table 2. Time consumed in different steps.

Modal frequency	Modal shape and pre-defined terms	Iteration of the driven point response			Cylinder velocity response
		Bilinear transform	DSS+MEM (Euler)	DSS+MEM (trapezoid)	
31.8 s	0.84 s	1.2 s	0.7 s	0.4 s	405 s

It is noticed that the proposed methods, especially the trapezoid approximate method, are more efficient than the bilinear transform method used by Avanzini. This phenomenon reveals that pre-calculation of two terms in Eq. (11) can efficiently reduce the computation cost. The fact that the trapezoid approximate method consumes less time than the Euler approximate method can be explained by the lower computational dimension of Newton–Raphson iterations than that of the DSS iterations.

4. Sound pressure calculation and comparison

4.1. Sound pressure calculation

A classical way to calculate the sound field of a cylinder is the continuous Raleigh integral method in cylindrical coordinate,[15] but it is too complex to meet the requirement of high computational efficiency. On the contrary, discrete Raleigh integral is more efficient since the computational dimension is greatly reduced by the discretization operation.[9,13] There are two discrete forms of Raleigh integrals in Eq. (7), i.e., the first order difference of velocity and the second order difference of displacement. The former discrete Raleigh integral form is adopted here for its lower computing cost. Another reason is that the velocity response of the structure can be calculated with DSS method rather than the FDTD method. The first order discrete Raleigh integral can be expressed as

$$P_j(n) = F_s \times \left(\boldsymbol{T}^{(a)}\right)^{\mathrm{T}} [\boldsymbol{V}(n) - \boldsymbol{V}(n-1)], \tag{21}$$

where P_j is the sound pressure at x_j, $\boldsymbol{V}$ and $\boldsymbol{T}^{(a)}$ are respectively the normal velocity vector of discrete surface nodes and the acoustic transfer vector. $\boldsymbol{V}$ and $\boldsymbol{T}^{(a)}$ can be described as follows;

$$\begin{cases} \boldsymbol{T}^{(a)} = \left\{ \dfrac{\rho_0}{2\pi \bar{r}_{ij}} \Delta S \right\}_i, \\ \boldsymbol{V}(n) = \{ v(i,j,U(n-1-\mathrm{Round}(\bar{r}_{ij} \cdot F_s/c_0)) \\ \qquad \times (n-1-\mathrm{Round}(\bar{r}_{ij} \cdot F_s/c_0)))\}_i, \end{cases} \tag{22}$$

where $\bar{r}_{ij}$ is the distance between the i-th structural surface node and the j-th sound field point, ΔS is the area of single surface element, $U(n)$ is the Heaviside function, and $\mathrm{Round}(x)$ rounds x to the nearest integer. The time delays of different elements are considered in Eq. (22). Suppose that the positions of a structural node and a sound field point are respectively (r_0, θ_i, z_i) and (r, θ_j, z_j), the distance $\bar{r}_{ij}$ can be obtained by

$$\bar{r}_{ij} = \sqrt{(r\sin\theta_j - r_0\sin\theta_i)^2 + (r\cos\theta_j - r_0\cos\theta_i)^2 + (z_j - z_i)^2}. \tag{23}$$

4.2. Result and validation

The receiving point of the sound field is set to $x_{\mathrm{recieve}}(r, \theta, z) = (2, 0, 0.08)$ and the impact sounds of different Raleigh integral forms are shown in Fig. 6. The solid line is the result of the proposed first order method and the dotted line is that of the second order FDTD method used by Lambourg and Zhang. Both of the results are based on the transient structural response calculated in Section 3.

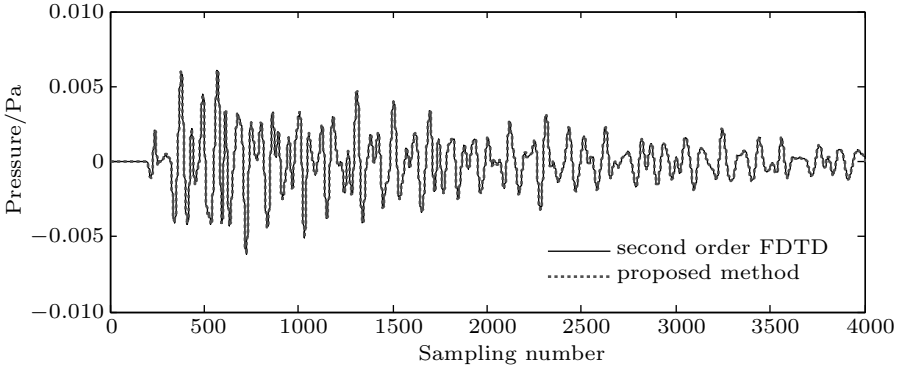


Fig. 6. Comparison of impact sounds from different Raleigh integral forms.

It is obvious that the impact sounds from different methods well agree with each other. The proposed first order method has the same accuracy to the second order FDTD method used by Lambourg and Zhang.

For further validation of the proposed impact sound synthesis method, the impact sound of a smaller cylinder ($L = 0.3$ $R = 0.1$) calculated respectively using FEM+MEM+BEM (realized through the transient modal superposition weakly coupled response case in Virtual.Lab software) and proposed method are shown in Fig. 7. It should be noted that the force obtained from Hertz contact process is used directly as the input force of the transient modal superposition structural weakly coupled response case. The result shows a good agreement between the two methods. The differences between the two methods can be explained by the calculation precision, the modal frequency bias, and the relative position of the driven point and the receiving point. In FEM, the precision is restricted to 6000 Hz for 10 mm mesh, meanwhile the cylinder structure is three-dimensioanl and it is difficult to keep the driven point exactly on the position expected when the mesh size is determined.

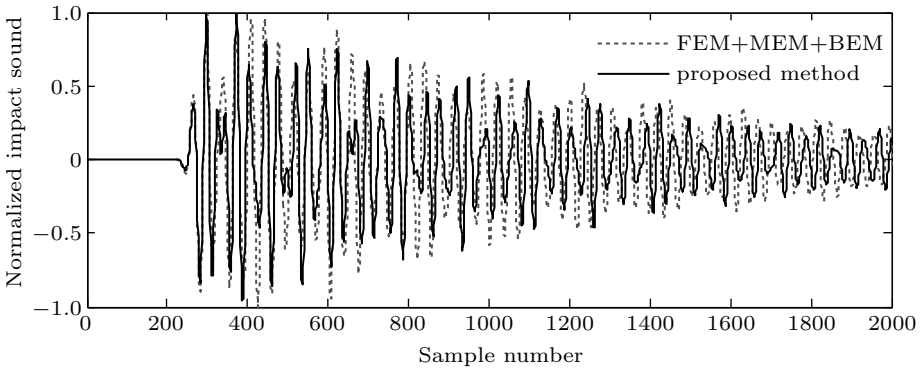


Fig. 7. Comparison of impact sounds from different impact sound synthesis methods.

4.3. Computation efficiency

The computing time of the impact sound (does not contain the Hertz contact and velocity response processes) is displayed in Table 3. As expected, the first order difference method is more efficient than the second order difference method and the BEM method in the calculation of impact sound. The computing time of the proposed first order method is less than half that of the second order FDTD method and the BEM method.

Table 3. Comparison of the impact sound computation efficiency.

Methods	Computing time of the impact sound/s
Proposed first order method ($L = 1.2$ $R = 0.4$)	98 (the first 0.1 s)
Second order FDTD method ($L = 1.2$ $R = 0.4$)	188 (the first 0.1 s)
Proposed first order method ($L = 0.3$ $R = 0.1$)	194.2 (the first 1 s)
BEM ($L = 0.3$ $R = 0.1$)	450.0 (the first 1 s)

5. Conclusion

Based on a simply supported cylindrical shell structure, an impact sound synthesis model comprising the Hertz contact process, the transient structural response process, and the sound radiation process is proposed. Firstly, the system equations are constructed through the modal extended DSS equations and the transient structural responses of the cylinder are obtained. Then the impact sound is calculated using the proposed first order discrete Rayleigh integral method. Finally, the sound synthesis model is verified in two steps: 1) verifying the structural response via the point admittance and FEM+MEM method, and 2) verifying the sound radiation by comparing impact sounds from different methods.

The results show that the DSS and MEM based sound synthesis model has advantages over the existing sound synthesis models in terms of both computational efficiency and accuracy. The sound synthesis model could provide a large number of effective sound samples for sound source identification study and could be easily transferred to the impact sound synthesis of other structures.

References

[1] Gaver W W 1993 *Ecol Psychol* **5** 1
[2] Chaigne A and Lambourg C 2001 *J. Acoust. Soc. Am.* **109** 1422
[3] Aramaki M, Besson M and Kronland-Martinet R 2011 *IEEE Trans. Audio Speech Lang. Processing* **19** 301
[4] Ashby M F, Brechet Y J M, Cebon D and Salvo L 2004 *Mater Design* **25** 51
[5] Chen K A, Tian X H and Yan S G 2017 *24th International Congress on Sound and Vibration*, July 23–27, 2017, London, United Kingdom, p. 1
[6] Liang Y, Chen K A and Zhang B R 2016 *Acta Acoustica* **41** 521 (in Chinese)
[7] Giordano B L and McAdams S 2006 *J. Acoust. Soc. Am.* **119** 1171

[8] Elie B, Gautier F and David B 2014 *J. Acoust. Soc. Am.* **136** 1385
[9] Lambourg C, Chaigne A and Matignon D 2001 *J. Acoust. Soc. Am.* **109** 1433
[10] Lutfi R A and Oh E L 1997 *J. Acoust. Soc. Am.* **102** 3647
[11] McAdams S, Roussarie V, Chaigne A and Giordano B L 2010 *J. Acoust. Soc. Am.* **128** 1401
[12] Zhang B R, Chen K A and Ding S H 2014 *Acta Phys. Sin.* **63** 217 (in Chinese)
[13] Zhang B R, Chen K A, Ma X Y and Ding S H 2014 *Acta Acoustica* **39** 75 (in Chinese)
[14] Avanzini F and Rocchesso D 2001 *Proc. Int. Computer Music Conf.*, La Habana, Cuba, p. 91
[15] Laulagnet B and Guyader J L 1994 *J. Acoust. Soc. Am.* **96** 277
[16] Freed D J 1990 *J. Acoust. Soc. Am.* **87** 311
[17] Hunt K H and Crossley F R E 1975 *Journal of Applied Mechanics* **42** 440
[18] Chen K A 2014 *Active Noise Control* (2nd Edn.) (Beijing: National Defense Industry Press) p. 44 (in Chinese)
[19] Hansen C, Snyder S, Qiu X J, Brooks L and Moreau D 2012 *Active Control of Noise and Vibration* (2nd Edn.) (Boca Raton: CRC Press) pp. 293–306
[20] Borin G, Poli G D and Rocchesso D 2000 *IEEE Trans. Audio Speech Lang. Processing* **8** 597